

# GEANT4 and PHITS simulations of the shielding of neutrons from $^{252}\text{Cf}$ source

Jae Won Shin,<sup>1</sup> Sang-In Bak,<sup>2</sup> Doyoon Kim,<sup>2</sup> Chong Yeal Kim,<sup>3</sup> and Seung-Woo Hong<sup>1,\*</sup>

<sup>1</sup>*Department of Physics, Sungkyunkwan University, Suwon 440-746, Korea*

<sup>2</sup>*Department of Energy Science, Sungkyunkwan University, Suwon 440-746, Korea*

<sup>3</sup>*Department of Radiation Science & Technology,  
Chonbuk National University, Jeonju 561-756, Korea*

(Dated: 26 March 2014)

## Abstract

Monte Carlo simulations by using GEANT4 and PHITS are performed for studying neutron shielding abilities of several materials, such as graphite, iron, polyethylene, NS-4-FR and KRAFTON-HB. As a neutron source  $^{252}\text{Cf}$  is considered. For the Monte Carlo simulations by using GEANT4, high precision (G4HP) models with G4NDL 4.2 based on ENDF/B-VII data are used. For the simulations by using PHITS, JENDL-4.0 library are used. The neutron dose equivalent rates with or without five different shielding materials are estimated and compared with the experimental values. It is found that the differences between the shielding abilities calculated by using GEANT4 with G4NDL 4.2 and PHITS with JENDL-4.0 library are not significant for all the cases considered in this work. We investigate the accuracy of the neutron dose equivalent rates obtained by GEANT4 and PHITS by comparing our simulation results with experimental data and other values calculated earlier. The calculated neutron dose equivalent rates agree well with the experimental dose equivalent rates within 20% errors except for polyethylene. For polyethylene material, discrepancy between our calculations and the experiments are up to 40%, but all simulations show consistent features.

PACS numbers: 07.05.Tp, 28.20.Fc, 02.70.Uu, 87.53.Bn

Keywords: Neutron shielding,  $^{252}\text{Cf}$ , GEANT4, PHITS, G4NDL 4.2, JENDL-4.0

---

\*Electronic address: swhong@skku.ac.kr

## I. INTRODUCTION

Accurate estimations of the neutron shielding abilities are essential for safety requirement in the design of facilities such as accelerators and nuclear reactors or a shielding container of neutron emitting sources. In determining the shielding abilities, characteristics of the materials is a major factor. Many studies have been done for neutron shielding abilities for various shielding materials [1–4], shielding designs [5–7], further development of new neutron shielding materials [8, 9] and etc. Also, benchmark simulations by using different Monte Carlo codes [10–17] have been done with MCNP, MCNP4B2, SAS, SCALE and GEANT4.

Effectiveness of various shielding materials for neutrons from a  $^{252}\text{Cf}$  source were experimentally evaluated in [4]. In Ref. [17], the neutron shielding was studied with GEANT4 code [18]. For neutron interactions, both high precision (G4HP) models with G4Neutron Data Library (G4NDL) 3.13 based on ENDF/B-VI library and low energy parameterized (G4LEP) models were used and tested. Relative neutron dose equivalent rates were calculated and the results were compared with the experimental data [4]. It was shown that G4HP models were a good candidate for accurate simulations of neutron shieldings.

As an extension of these previous studies [10–17], we have performed in this work Monte Carlo simulations for neutron shielding by using GEANT4 and PHITS [19–21]. In Ref. [17] G4NDL 3.13 based on ENDF/B-VI was used for GEANT4 v9.3, but the latest version of nuclear data available for GEANT4 is now G4NDL 4.X based on ENDF/B-VII. In this work, we also used different Monte Carlo code PHITS for a benchmark purpose. For neutron interactions, G4HP models with G4NDL 4.2 based on ENDF/B-VII library and JENDL-4.0 library are used for GEANT4 v9.6 and PHITS v2.52 simulations, respectively. As a neutron source,  $^{252}\text{Cf}$  is assumed.  $^{252}\text{Cf}$  emits neutrons with an average energy of  $\sim 2.2$  MeV by spontaneous fission. In Ref. [3, 4] the neutron dose equivalent rates are extracted instead of measuring neutron spectrum. Thus, we also estimated the neutron dose equivalent rates for comparison with the experimental results [3, 4]. The neutron dose equivalent rates with and without the shield are estimated for shielding materials such as graphite, iron, polyethylene, NS-4-FR and KRAFTON-HB. Graphite is used in reactor design as a moderator and reflector. Iron is commonly used for the high energy neutron shielding in accelerator facilities. Polyethylene is a popular neutron shielding material that highly

contains hydrogen. NS-4-FR is an epoxy resin containing heavy elements together with boron to reduce the production of secondary  $\gamma$ -rays due to thermal neutron absorption. KRAFTON-HB also contains boron for the same purpose, and was developed as an advanced shielding material for fast breeder reactors. By comparing our results with the experimental data [3, 4] and the previous simulation results [10, 12, 14], we can compare the accuracy of the neutron dose equivalent rates obtained by GEANT4 and PHITS with new nuclear data libraries.

The outline of the paper is as follows. In Sec. II, simulation tools and simulation set up are described. In Sec. III, the calculated neutron energy distributions scored in the detector region and the corresponding neutron dose equivalent rates are shown. The resulting neutron dose equivalent rates are compared with experimental data. A summary is given in Sec. IV.

## II. METHOD

### A. Simulation tools

As Monte Carlo simulation tools, we use GEANT4 and PHITS and compare the results from them. For the low energy neutron interactions in material, G4HP models with G4NDL based on ENDF library [22] and JENDL library [23] are used in GEANT4 and PHITS simulations, respectively. Here we list some key features of the simulation tools.

**GEANT4 :** GEANT4 (GEometry ANd Tracking) is a simulation tool kit written in C++ language, which allows microscopic simulations of the propagation of particles interacting with materials. It is being widely used in many different fields, such as neutron shielding studies [17, 24], medical physics [25–28], accelerator based single event upset studies [29, 30], environment radiation detection studies [31–33], and etc.

In our previous work [17], we showed that G4HP models with G4NDL 3.13 were better than G4LEP models. For this reason, G4HP models with G4NDL 4.2 are used in this work. Both G4HP models and G4LEP models include cross sections for elastic, inelastic scattering, capture, fission and isotope production. The energy range of these classes are from thermal energies to 20 MeV. Data of G4NDL 4.2 come largely from the ENDF/B-VII library. The validations and the detailed descriptions of the GEANT4, G4HP models and G4NDL can be found on the GEANT4 website [34].

PHITS : PHITS (Particle and Heavy-Ion Transport code System) is a multi-purpose Monte Carlo transport code system for heavy ions and all particles with the energies from meV up to 200 GeV. It was developed by the collaboration of Japan Atomic Energy Agency (JAEA), Research Organization for Information Science Technology (RIST), High Energy Accelerator Research Organization (KEK), and several other institutes. PHITS is also used for many scientific studies such as space technology [35, 36], medical physics [37–39], shielding designs [7, 40, 41], accelerator applications [42, 43] and etc.

Neutron simulations can be done by using various evaluated nuclear data libraries in PHITS code. JENDL-4.0 library, which is the latest version of JENDL, is used in this work. Additional information and detailed descriptions of PHITS can be found on the web [44].

## B. Simulation set up

In this work, we consider the neutron shielding experiments in Ref. [3, 4], where the experiments were done to evaluate the effectiveness of various shielding materials for neutrons from a  $^{252}\text{Cf}$  source.  $^{252}\text{Cf}$  emits neutrons with an average energy of  $\sim 2.2$  MeV. For the generation of neutrons from  $^{252}\text{Cf}$  source, Watt fission spectrum [45–47] are used in our simulations. The spontaneous fission neutron spectrum given by the Watt fission spectrum is expressed as

$$f(E) = \exp\left(-\frac{E}{1.025}\right)\sinh(2.926E)^{1/2}, \quad (1)$$

where  $E$  is the neutron energy in MeV [47].

The geometry of the shield and the detector is drawn in Fig. 1. The  $^{252}\text{Cf}$  source is surrounded by a  $50 \times 50 \times 50$  cm<sup>3</sup> paraffin container block. There is a conical shape of an opening in the paraffin so that the neutrons from the  $^{252}\text{Cf}$  can pass freely and propagate through the air to reach the detector behind the shield. The neutron detector has a cylindrical shape of radius 5.25 cm and length 10 cm. It is assumed that all the neutrons that reach the detector are scored. Shielding materials, source strengths of  $^{252}\text{Cf}$ , d1, d2 and the thicknesses ( $t$ ) of the shielding materials are tabulated in Table I. Five different shielding materials such as graphite, iron, polyethylene, NS-4-FR and KRAFTON-HB are considered. The components of these materials and their mass fractions are tabulated in Table II.

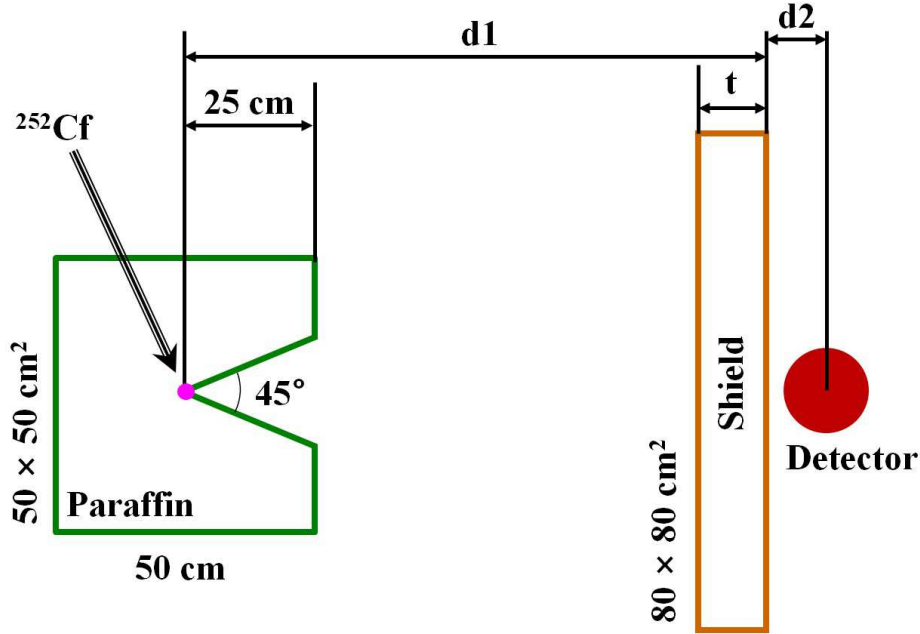


FIG. 1: Schematic diagram showing the simulation geometry.

TABLE I: Parameters for the neutron shielding experiments and simulations used in this work

materials	neutron source strength (n/sec)	d1 (cm)	d2 (cm)	t (cm)
Graphite [3]	$1.62 \times 10^7$	90	20	5, 15, 25, 35
Iron [3]	$1.50 \times 10^7$	90	20	5, 15, 25, 35
Polyethylene [3]	$6.28 \times 10^7$	90	20	5, 15, 25, 35
NS-4-FR [4]	$5.45 \times 10^7$	100	15	5, 10, 15, 20, 25
KRAFTON-HB [4]	$5.45 \times 10^7$	100	15	5.3, 10.6, 15.9, 21.2, 26.5, 31.8

Typical simulation snap shots drawn by using OpenGL library are shown in Fig. 2. Figures 2 (a) and 2 (b) show the propagation of neutrons and gammas without and with the shielding material, respectively. It can be seen that a large number of neutrons fly through the opening but are mostly blocked by the shielding material. With this geometry, the energy distributions of the neutrons scored in the detector after escaping through the shielding materials are calculated.

To make a comparison with the experimental results given in terms of dose equivalent rates [3, 4], we need to calculate dose equivalent rates. To estimate the human biological dose equivalent rates, one often uses a conversion factor which converts the neutron flux

TABLE II: Components and mass fractions of shielding materials used in this work

	graphite	iron	polyethylene	NS-4-FR	KRAFTON-HB
H	-	-	14.4	5.92	10.66
B	-	-	-	0.94	0.78
C	100	-	85.6	27.63	75.29
N	-	-	-	1.98	2.20
O	-	-	-	42.29	10.69
Al	-	-	-	21.24	-
Si	-	-	-	-	0.38
Fe	-	100	-	-	-

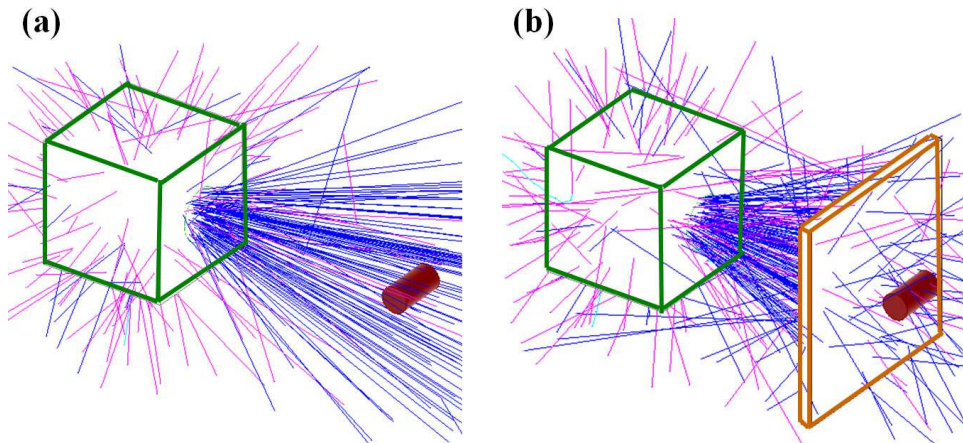


FIG. 2: (Color online) OpenGL pictures showing the simulation geometry and the neutrons (blue) and gammas (pink) without (a) and with (b) the shielding.

to human biological dose equivalent rate. In this work, neutron dose equivalent rates are calculated by using the flux to dose conversion factor from the National Council on Radiation Protection and Measurements (NCRP-38) standard [48].

### III. RESULTS

Simulations are performed by using GEANT4 v9.6 with G4NDL 4.2 and PHITS v2.52 with JENDL-4.0. First, the calculated neutron energy spectra scored in the detector region for various shielding materials are shown. The scored numbers of neutrons are normalized

by the number of neutrons generated by the source. We refer to these values as "counts". In Ref. [17], the neutron shielding simulations were done by using GEANT4 v9.3 with G4NDL 3.13. The data of G4NDL 3.13 are based on the ENDF/B-VI library. For the comparison between the results of Ref. [17] and the present work, the calculations by using GEANT4 v9.3 with G4NDL 3.13 have been also performed and the results are compared. The results from GEANT4 v9.6 with G4NDL 4.2 and PHITS v2.52 with JENDL-4.0 are also compared with each other.

The calculated the neutron dose equivalent rates by using the flux to dose conversion factor from NCRP-38 are compared with those from the experiments [3, 4] and other values calculated earlier [10, 12, 14].

### **A. Neutron spectra scored in the detector region**

Neutron spectra scored in the detector region obtained from GEANT4 with G4NDL 3.13 and G4NDL 4.2 and those from PHITS with JENDL-4.0 are compared with each other. However, differences among the simulation results are not significant for all the cases. For this reason, we show only the results from GEANT4 v9.6 with G4NDL 4.2 and PHITS v2.52 with JENDL-4.0. For brevity, we refer to the calculations by using GEANT4 v9.6 with G4NDL 4.2 and PHITS v2.52 with JENDL-4.0 as simply GEANT4 and PHITS, respectively.

Figure 3 shows the energy distributions of the neutrons scored in the detector region after passing through the shielding materials. The results for five different shielding materials with 15 and 25 cm of thicknesses are plotted in Fig. 3 (a) and 3 (b), respectively. It can be seen that graphite and iron reduce the number of neutrons at high energies but not at low energies in comparison with the counts without any shielding material. Also, graphite and iron do not reduce the neutron flux as much as other shielding materials. For polyethylene, NS-4-FR and KRAFTON-HB, which contain the hydrogen element, similar shapes of the spectrum and neutron shielding abilities are observed. It can be seen that those materials reduce the counts by up to two orders of magnitudes in comparison with the counts without any shielding material.

Peak and valley structures are observed for both graphite and iron materials in Fig. 3, which can be understood from the total cross sections of the neutron on the elements. Figure 4 shows the energy distributions of the neutrons and the total cross sections of the

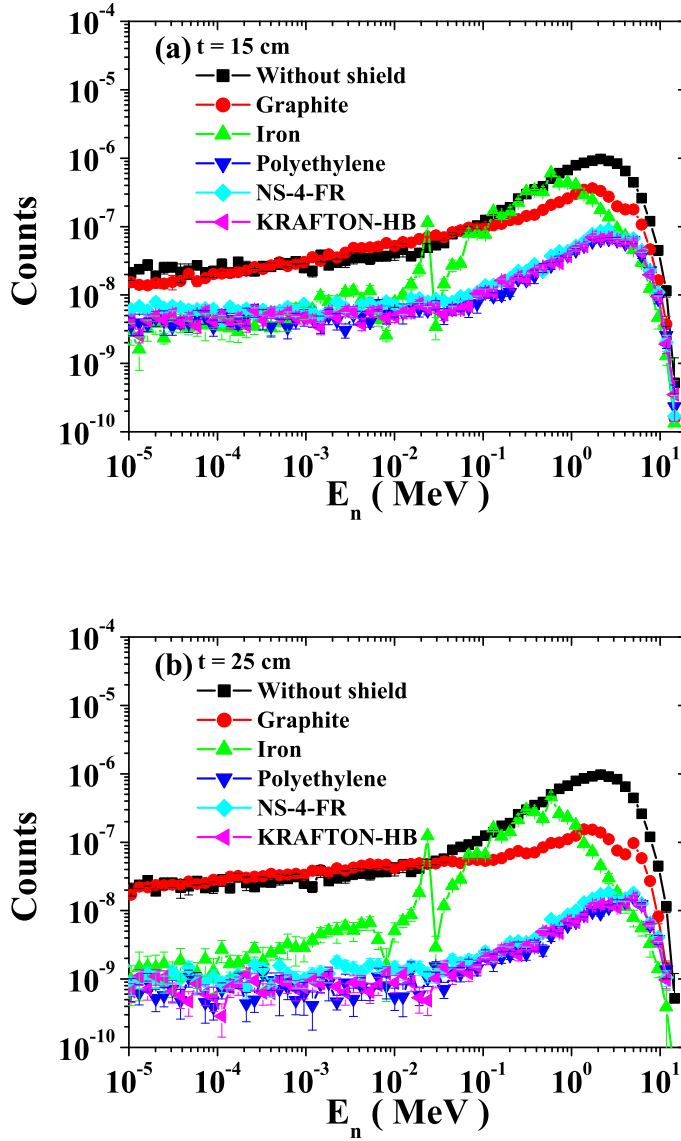


FIG. 3: (Color online) Energy distributions of the neutrons scored in the detector region for various shielding materials. (a) and (b) show the results for the 15 and 25 cm of the shielding thickness, respectively.

neutron on the elements of the shielding materials. Total cross sections of the neutron on  $^{nat}\text{C}$ ,  $^{54}\text{Fe}$ ,  $^{56}\text{Fe}$ ,  $^{57}\text{Fe}$  and  $^{58}\text{Fe}$  are taken from ENDF/B-VII.1 [22]. Figure 4 (a) shows the energy distributions of the neutrons scored in the detector region with and without graphite materials and the total cross section of the neutron on  $^{nat}\text{C}$ . As the thickness of the graphite material increases, the valley of the neutron spectrum near  $\sim 3.5$  MeV becomes pronounced.



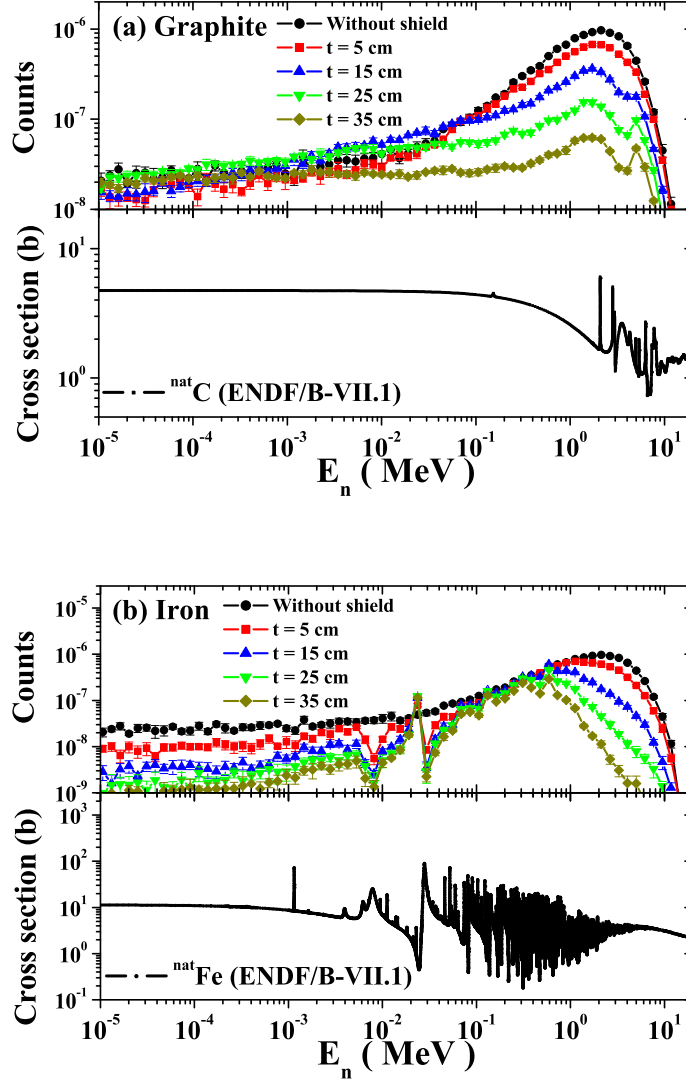


FIG. 4: (Color online) (a) and (b) represent the results for graphite and iron shielding materials, respectively. The upper panels show energy distributions of the neutrons in the detector regions and the lower panels show the total cross sections of the neutron on graphite and iron. Total cross sections are taken from ENDF/B-VII.1 library [22].

This feature can be understood by the total cross section of the neutron on  $^{nat}\text{C}$  plotted in the lower panel. A broad peak, which mainly comes from the elastic cross section of the neutron on  $^{nat}\text{C}$ , is shown near  $\sim 3.5$  MeV [22]. As a result, the neutrons with these energies are more reduced than those with other neutrons.

For iron, drastic changes are observed in Fig. 4 (b). Two distinct valleys (at  $\sim 0.008$  and

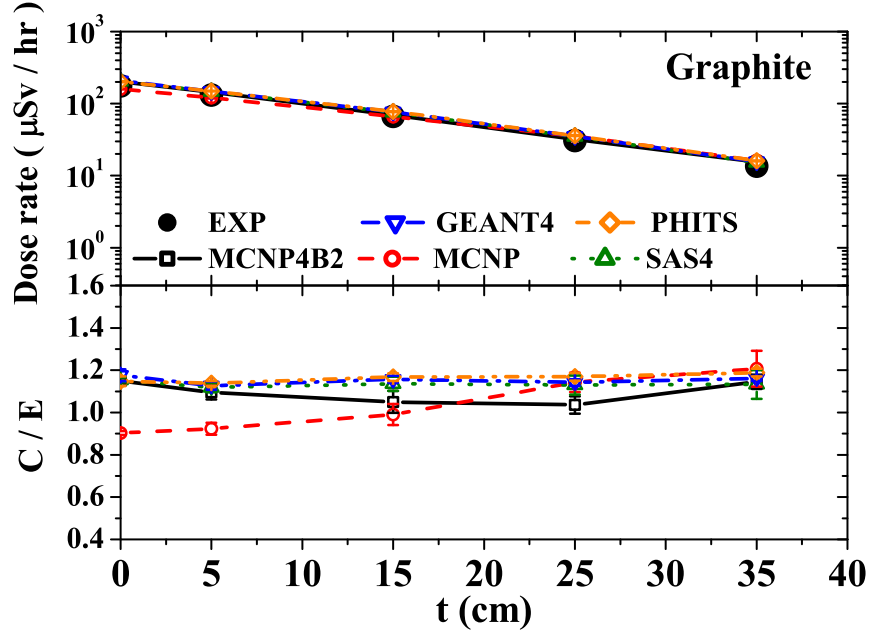


FIG. 5: (Color online) Neutron dose equivalent rates for graphite. The upper panel shows the dose equivalent rates in units of  $\mu\text{Sv/hr}$ , and the lower panel shows the ratio of the calculated dose equivalent rates to the experimental dose equivalent rates. The filled circles represent the experimental dose equivalent rates [3]. The open inverted triangles and the diamonds represent the calculated dose equivalent rates by using GEANT4 and PHITS, respectively. The open squares, circles and triangles denote the calculated dose equivalent rates by using MCNP4B2 [12], MCNP [10] and SAS4 [10], respectively.

$\sim 0.03$  MeV) and one peak ( $\sim 0.024$  MeV) are shown. One can see that the energy distribution looks similar to a mirror image of the total cross section of the neutron on  $^{nat}\text{Fe}$ . The peaks at  $\sim 0.008$  and  $\sim 0.03$  MeV in the lower panel mainly come from the contributions from elastic cross section of the neutron on  $^{54}\text{Fe}$  and  $^{56}\text{Fe}$ , respectively [22]. Also, a very sharp peak at  $\sim 0.00115$  MeV which comes from the contribution of capture cross section of the neutron on  $^{56}\text{Fe}$  [22] is shown in the lower panel. However, the probability that neutrons reach the energies of those sharp peak is very low because the peak has a very narrow width  $< \sim 10$  eV. For this reason, this sharp peak at  $\sim 0.00115$  MeV does not produce a visible effect on the neutron counts.

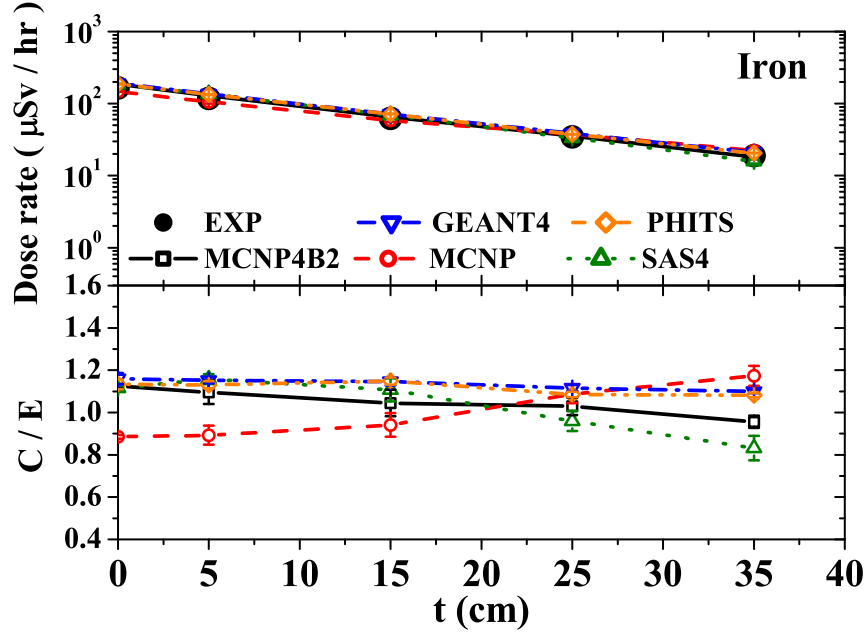


FIG. 6: (Color online) The same as in Fig. 5 except that the material is iron.

### B. Neutron dose equivalent rates

With the energy distributions of the neutrons scored in the detector region and the conversion factors from NCRP-38, we can obtain neutron dose equivalent rates. Figures 5 ~ 9 show our results for the experimental dose equivalent rates for five different shielding materials. The upper and lower panels of each figure represent the dose equivalent rates in units of  $\mu\text{Sv/hr}$  and the ratio of the calculated values to the experimental values (C/E) [3, 4], respectively.

Figures 5 and 6 show the neutron dose equivalent rates for graphite and iron shielding materials, respectively. One can see that all the calculations agree with the experiments within  $\sim 20\%$  errors. C/E from both GEANT4 and PHITS are almost independent of thicknesses of the shielding materials. It means that the calculated neutron dose attenuations are very close to those from the experiments.

For polyethylene, discrepancies between the experimental values and the simulations values are up to  $\sim 40\%$  as shown in Fig. 7. All simulations overestimate the experimental dose equivalent rates. Similar features can be seen in Ref. [15]. In Ref. [15], even though

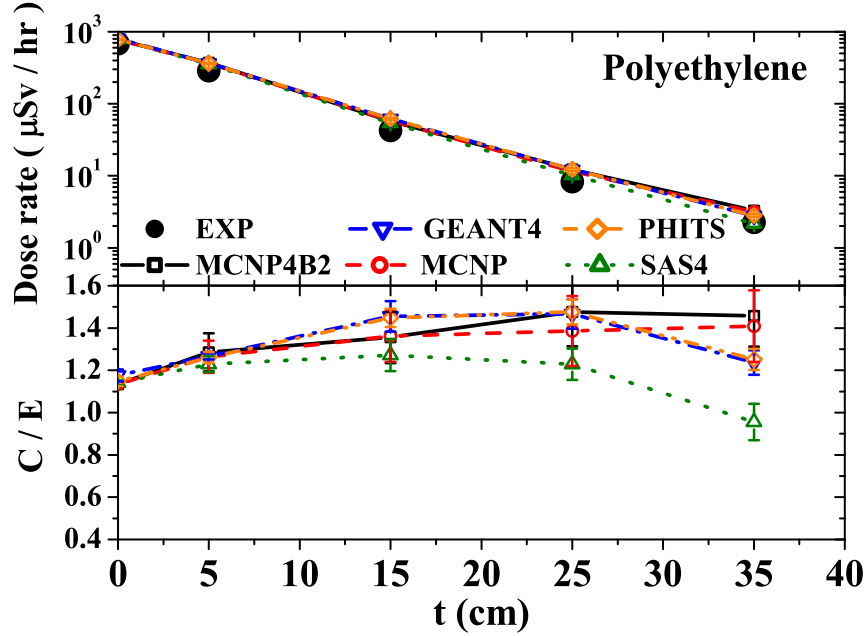


FIG. 7: (Color online) The same as in Fig. 5 but for polyethylene.

differences between the calculated dose equivalent rates and the measured one for NS-4-FR and KRAFTON-HB were less than  $\sim 20\%$ , the calculated dose equivalent rates overestimated the experimental values up to  $\sim 50\%$  for polyethylene.

Neutron dose equivalent rates for NS-4-FR and KRAFTON-HB are plotted in Fig. 8 and Fig. 9, respectively. One can see that the calculated neutron dose equivalent rates agree well with the experimental dose equivalent rates within  $\sim 10\%$  errors. Also, differences among the calculations are not significant.

Figure 10 shows the neutron dose attenuations for five shielding materials considered in this work. The filled symbols and open symbols with lines denote the experimental and the calculated neutron dose attenuations, respectively. Only the results from GEANT4 are denoted in this figure, because differences between the results from GEANT4 and PHITS are not significant. Both the experiments and our simulations show the same trend in this figure. As mentioned before, the calculated and the experimental values for both graphite and iron almost overlap with each other within  $\sim 5\%$  errors. The differences between the calculated and the experimental values for polyethylene, NS-4-FR and KRAFTON-HB are within  $\sim 30\%$ ,  $\sim 10\%$  and  $\sim 10\%$  errors, respectively.

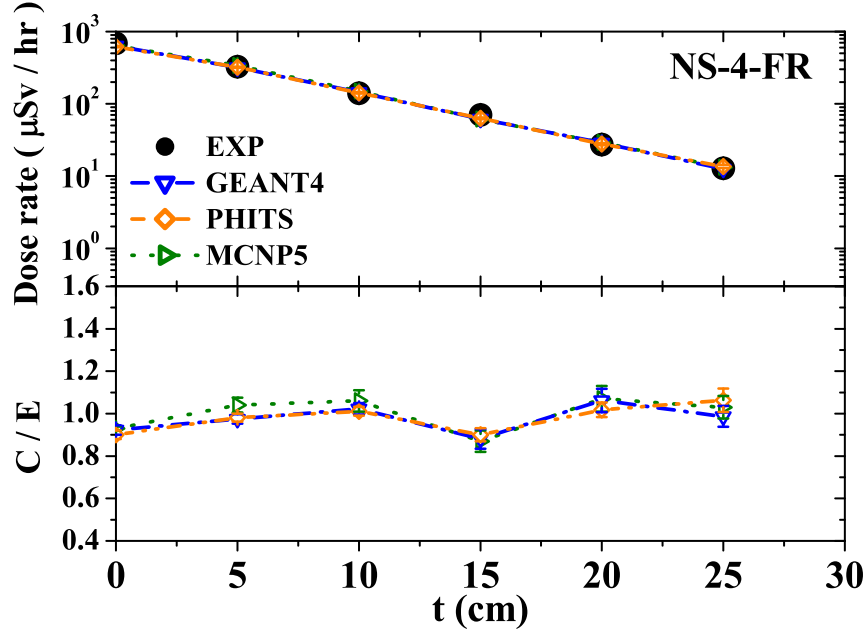


FIG. 8: (Color online) Neutron dose equivalent rates for NS-4-FR. The upper panel shows the dose equivalent rates in units of  $\mu\text{Sv/hr}$ , and the lower panel shows the ratio of the calculated dose equivalent rates to the experimental dose equivalent rates. The filled circles represent the experimental dose equivalent rates [4]. The open inverted triangles and diamonds represent the calculated dose equivalent rates by using GEANT4 and PHITS, respectively. The open triangles denote the calculated dose equivalent rates by using MCNP5 [14].

In Fig. 10, it can be seen that both graphite and iron materials reduce the neutron dose up to one order of magnitude when the thickness is 35 cm. Even though the energy distributions of the neutrons for graphite differ from those for iron as can be seen in Fig. 4, the neutron dose attenuation for graphite is almost the same as that for iron at  $t = 5$  cm and 15 cm. As the thickness of the shield increases, however, difference between the attenuations for graphite and iron become significant. When polyethylene, NS-4-FR and KRAFTON-HB shielding materials are used, doses are reduced very effectively compared to graphite and iron. Shielding abilities of polyethylene, NS-4-FR and KRAFTON-HB with 15 cm of thickness are comparable to or better than those of graphite and iron with 35 cm of thickness. When the thickness of the shielding materials is larger than 25 cm, neutron doses are reduced by two orders of magnitudes.

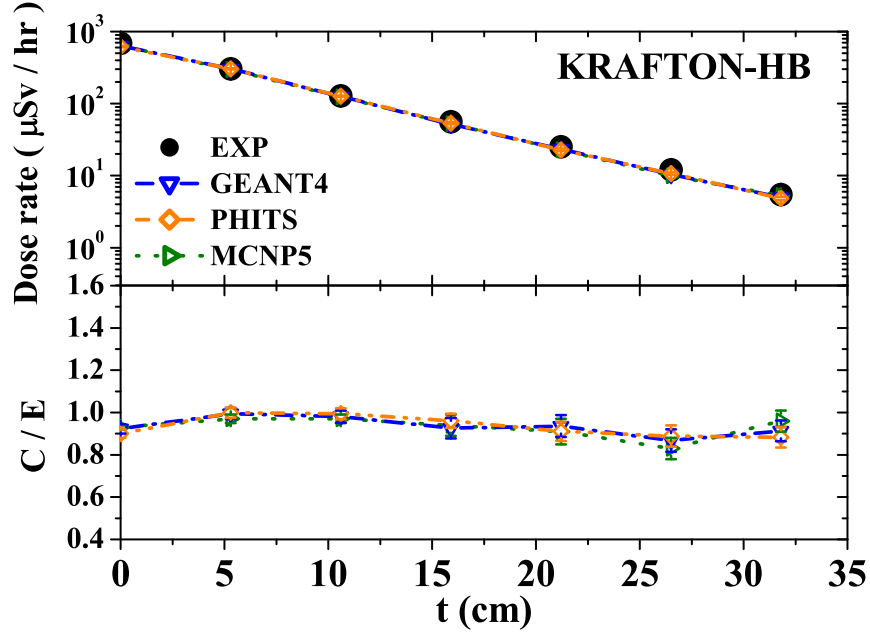


FIG. 9: (Color online) The same as in Fig. 8 but for KRAFTON-HB.

#### IV. SUMMARY

Neutron dose equivalent rates for various shielding materials are calculated by using GEANT4 and PHITS code. As a neutron source,  $^{252}\text{Cf}$  is assumed. Five different shielding materials such as graphite, iron, polyethylene, NS-4-FR and KRAFTON-HB are considered. For low energy neutron interactions, G4HP models with G4NDL 4.2 based on ENDF/B-VII and JENDL-4.0 library are used for GEANT4 and PHITS calculations, respectively.

First, the neutron energy distributions scored in the detector region with and without shielding materials are calculated. The results obtained from GEANT4 and PHITS are compared with each other. Also, an old version of GEANT4 and G4NDL 3.13 based on ENDF/B-VI as in [17] are considered and the results are compared. It is found that differences between the calculations from GEANT4 and PHITS and the difference between the old and new versions of GEANT4 are not significant for all the cases considered in this work, which shows reliability of these Monte Carlo simulations.

Second, the neutron dose equivalent rates with the calculated neutron spectra and conversion factors are obtained. The results are compared with the experimental dose equivalent

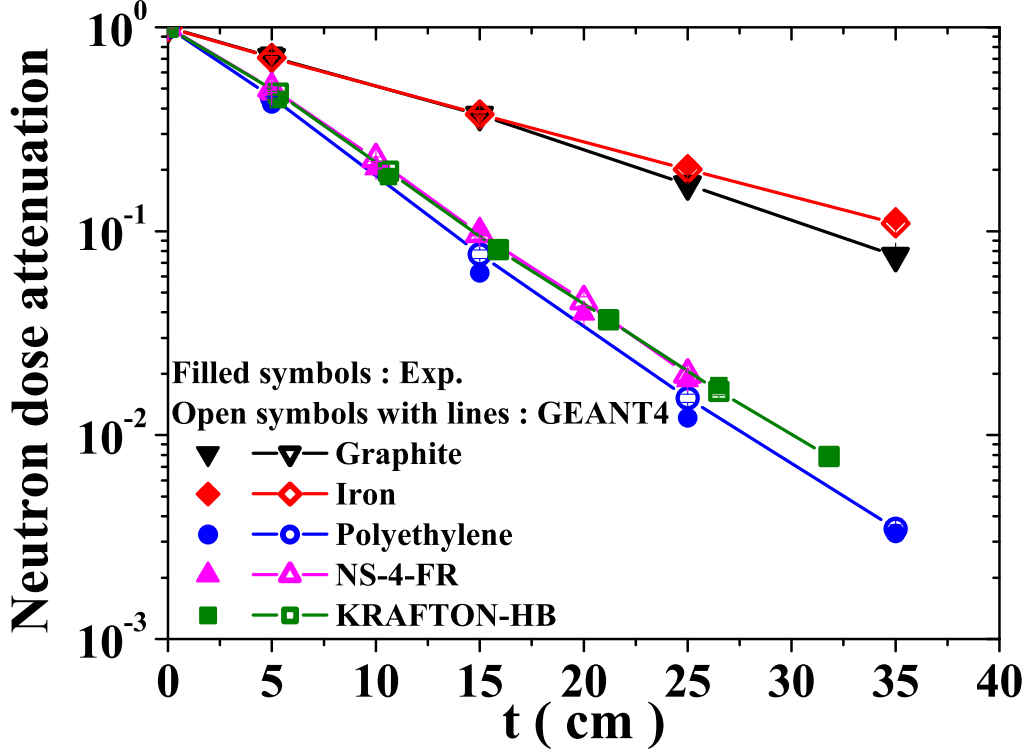


FIG. 10: (Color online) Neutron dose attenuations for graphite, iron, polyethylene, NS-4-FR and KRAFTON-HB are plotted as a function of thickness  $t$ . The filled symbols and open symbols with lines denote the experimental and the calculated neutron dose attenuations, respectively.

rates [3, 4] and the values calculated earlier [10, 12, 14]. From the comparison, it is found that GEANT4 and PHITS results based on nuclear data libraries describe the experimental dose equivalent rates quite well for the graphite, iron, NS-4-FR and GRAFTON-HB with the discrepancy between the experimental dose equivalent rates and the calculated values less than  $\sim 20\%$ . However, in the case of polyethylene, the discrepancy is up to  $\sim 40\%$ . Other studies [10, 12, 15] as well as the present study show consistent features.

Neutron dose attenuations for the shields are also obtained. For graphite or iron shielding materials, the simulation results are consistent with the experiments within  $\sim 5\%$  errors. The differences between the simulations and the experiments for polyethylene, NS-4-FR and KRAFTON-HB are less than  $\sim 30\%$ ,  $\sim 10\%$  and  $\sim 10\%$ , respectively.

## Acknowledgments

This work was supported in part by the Basic Science Research Program through the Korea Research Foundation (NRF-2011-0025116, NRF-2012R1A1A2007826, NRF-2012M2B2A4030183).

---

- [1] K. Ueki and Y. Namito, Nucl. Sci. Eng. **96**, 30 (1987).
- [2] K. Ueki and Y. Namito, J. Nucl. Sci. Technol. **26**, 411 (1989).
- [3] K. Ueki, A. Ohashi and Y. Anayma, in *Proceedings of New Horizons in Radiation Protection and Shielding Topical Meeting*, (Pasco, Washington, USA, April 26-May 1, 1992), p. 130-137.
- [4] K. Ueki *et al.*, Nucl. Sci. Eng. **124**, 455 (1996).
- [5] J. C. Liu and T. T. Ng, Radiat. Prot. Dosim. **83**, 257 (1999).
- [6] A. X. da Silva and V. R. Crispim, Radiat. Prot. Dosim. **95**, 333 (2001).
- [7] D. Satoh *et al.*, J. Nucl. Sci. Technol. **49**, 1097 (2012).
- [8] K. Okuno, Radiat. Prot. Dosim. **115**, 258 (2005).
- [9] A. M. Sukegawa *et al.*, J. Nucl. Sci. Technol. **48**, 585 (2011).
- [10] H. Taniuchi and B. L. Broadhead, in *ANS 8th International Conference on Radiation Shielding*, (Arlington, Texas, USA, April 24-27, 1994).
- [11] B. L. Broadhead, J. S. Tang, R. L. Childs, C. V. Parks and H. Taniuchi, Nucl. Technol. **117**, 206 (1997).
- [12] "SOFTWARE QUALIFICATION REPORT for MCNP Version 4B2 - A General Monte Carlo N-Particle Transport Code", 30033-2003 Rev 01, 1998.
- [13] M. Bace, R. Jecmenica and T. Smuc, in *International Conference Nuclear Energy in Central Europe '99*, (Portoroz, Slovenia, September 6-9, 1999), p. 75-81.
- [14] D. A. Torres, R. D. Mosteller and J. E. Sweezy, LA-UR-04-0122, Los Alamos National Lab., 2004.
- [15] D. Wiarda, M. E. Dunn, D. E. Peplow, T. M. Miller and H. Akkurt, NUREG/CR-6990, Oak Ridge National Laboratory, 2009.
- [16] D. E. Peplow, Nucl. Technol. **174**, 289 (2011).
- [17] S. I. Bak, T. S. Park, S. W. Hong, J. W. Shin and I. S. Hahn, J. Korean Phys. Soc. **59**, 2071



- (2011).
- [18] S. Agostinelli *et al.*, Nucl. Instrum. Methods Phys. Res. Sect. A **506**, 250 (2003).
  - [19] H. Iwase, K. Niita and T. Nakamura, J. Nucl. Sci. Technol. **39**, 1142 (2002).
  - [20] K. Niita *et al.*, Radiat. Meas. **41**, 1080 (2006).
  - [21] T. Sato *et al.*, J. Nucl. Sci. Technol. **50**, 913 (2013).
  - [22] <http://www.nndc.bnl.gov/csewg/>.
  - [23] <http://wwwndc.jaea.go.jp/jendl/jendl.html>.
  - [24] S. Avery, C. Ainsley, R. Maughan and J. McDonough, Radiat. Protect. Dosim. **131**, 167 (2008).
  - [25] G. Barca *et al.*, Nucl. Phys. B Proc. Suppl. **125**, 80 (2003).
  - [26] M. U. Bug *et al.*, Eur. Phys. J. D **60**, 85 (2010).
  - [27] J. W. Shin, S. W. Hong, C. I. Lee and T. S. Suh, J. Korean Phys. Soc. **59**, 12 (2011).
  - [28] arXiv:1401.0692v1.
  - [29] J. K. Park *et al.*, J. Korean Phys. Soc. **58**, 1511 (2011).
  - [30] J. W. Shin *et al.*, J. Korean Phys. Soc. **59**, 2022 (2011).
  - [31] S. Hurtado, M. Garcia-Leon and R. Garcia-Tenorio, Nucl. Instr. and Meth. A **518**, 764 (2004).
  - [32] K. Banerjee *et al.*, Nucl. Instr. and Meth. A **608**, 440 (2009).
  - [33] P. M. Joshirao *et al.*, Appl. Radiat. Isot. **81**, 184 (2013).
  - [34] <http://geant4.web.cern.ch/>.
  - [35] T. Sato and K. Niita, Radiat. Res. **166**, 544 (2006).
  - [36] A. A Bahadori *et al.*, Phys. Med. Biol. **58**, 7183 (2013).
  - [37] H. Nose, Y. Kase, N. Matsufuji and T. Kanai, Med. Phys. **36**, 870 (2009).
  - [38] T. Sato, Y. Kase, R. Watanabe, K. Niita and L. Sihver, Radiat. Res. **171**, 107 (2009).
  - [39] E. Seravalli *et al.*, Phys. Med. Biol. **57**, 1659 (2012).
  - [40] Y. Iwamoto and R. M. Ronningen, Nucl. Instr. and Meth. B **269**, 353 (2011).
  - [41] A. M. Sukegawa, H. Kawasaki and K. Okuno, Prog. Nucl. Sci. Technol. **2**, 375 (2011).
  - [42] A. N. Golovchenko *et al.*, Radiat. Meas. **45**, 856 (2010).
  - [43] Y. Iwamoto *et al.*, Nucl. Instr. and Meth. A **629**, 43 (2011).
  - [44] <http://phits.jaea.go.jp/>.
  - [45] B. E. Watt, Phys. Rev. **87**, 1037 (1952).
  - [46] A. B. Smith, P. R. Fields and J. H. Roberts, Phys. Rev. **108**, 411 (1957).

- [47] X-5 MONTE CARLO TEAM, LA-UR-03-1987, Los Alamos National Lab., 2003.
- [48] National Council on Radiation Protection and Measurements Protection Against Neutron Radiation NCRP Report 38.